Journal of Alloys and Compounds 509 (2011) 2734–2737

Contents lists available at ScienceDirect

Journal of Alloys and Compounds

journal homepage: www.elsevier.com/locate/jallcom

Review

Microwave complex permeability of planar anisotropy carbonyl-iron particles

Rui Han, Liang Qiao, Tao Wang*, Fa-shen Li*

Institute of Applied Magnetics, Key Laboratory of Magnetism and Magnetic Materials of the Ministry of Education, Lanzhou University, Lanzhou 730000, People's Republic of China

ARTICLE INFO

Article history:
Received 5 July 2010
Received in revised form
11 November 2010
Accepted 12 November 2010
Available online 20 November 2010

Key words:
Planar anisotropy carbonyl-iron (PACI)
Demagnetizing field
Complex permeability
Rotational orientation

ABSTRACT

Planar anisotropy carbonyl-iron (PACI) particles were prepared from sphere-shaped carbonyl-iron (SSCI) materials by a simple ball milling technique. The frequency-dependent complex permeability of paraffin composites with 50% volume concentration of particles has been investigated in 0.1–18 GHz frequency range. The as-milled PACI composites show a dramatic enhancement of complex permeability and a higher resonance frequency compared with SSCI composite. This is due to the PACI particles, which have an easy magnetization plane and a thickness smaller than their skin depth, suppressing the eddy current effects. Furthermore, the complex permeability is further improved after the PACI composite was rotationally orientated in an external magnetic field. The real permeability of oriented PACI composite reaches a large value of approximate 10.5 at 0.1 GHz, and the resonance frequency shifts to a higher frequency range.

Contents

1. Introduction

In recent years, electromagnetic (EM) wave devices over the gigahertz (GHz) frequency range have been widely used in both civil and military applications: personal digital assistants, local area net works, wireless communication tools, radar, etc. However, the increasing usage of EM-wave devices results in serious electromagnetic interference (EMI) and electromagnetic compatibility (EMC) problems. A good way to overcome these problems is exploiting a type of microwave-absorbing materials with strong absorption [1–5].

Among all of microwave absorbing materials, metallic magnetic materials are especially focused on because their permeability still remains high in GHz range due to their high saturation magnetization [6]. As we all know, the high-frequency behavior of metallic magnetic materials can be well described by Snoek's limit [7,8]:

$$(\mu_s - 1)f_r = \frac{1}{3\pi}\gamma M_s. \quad (1)$$

The right part of the expression is defined as Snoek's constant, where γ is the gyromagnetic ratio and M_s is the saturation magnetization. This limit demonstrates that it is impossible to enhance the static permeability (μ_s) and resonance frequency (f_r) at the same time. However, the easy-plane anisotropy picture provides us a new approach to exceed Snoek's limit. Based on the Landau–Lifshitz–Gilbert (LLG) equation [9], no matter what is the precise origin of the anisotropy, the precession of the magnetization around the easy axis in any magnetic materials can be determined by the anisotropy fields acting on the magnetization. The fundamental condition of the easy-plane anisotropy picture is that there is an easy magnetization plane in the magnetic particles, and hence there are two anisotropy fields H_{ha} and H_{ea} which are the effective anisotropy fields when the magnetization deviates from the easy axis (x direction) in the hard plane (x–z) and in the easy plane (x–y), respectively, as shown in Fig. 1 [10].

Based on the Landau–Lifshitz–Gilbert (LLG) equation, the product of μ_s and f_r for easy-plane anisotropy materials is obtained [9,10]:

$$(\mu_s - 1)f_r = \frac{\gamma M_s}{2\pi}\sqrt{\frac{H_{ha}}{H_{ea}}} \quad (2)$$

* Corresponding authors.
E-mail addresses: wtao@lzu.edu.cn (T. Wang), lifs@lzu.edu.cn (F.-s. Li).

0925-8388/$ – see front matter © 2010 Elsevier B.V. All rights reserved.
doi:10.1016/j.jallcom.2010.11.074

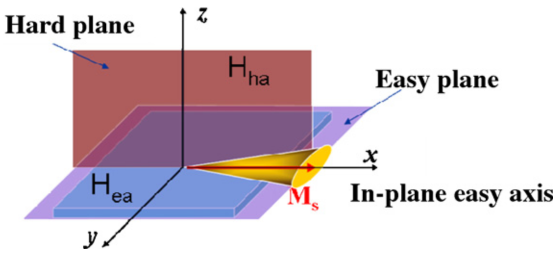

Fig. 1. Scheme of the precession of magnetization under the easy-plane anisotropy picture.

Compared with Eq. (1), the product of μ_s and f_r for easy-plane anisotropy materials is much larger than that of isotropy particles because of $H_{ha} \gg H_{ea}$. For PACI particles, the shape anisotropy plays an important role in the total anisotropy. Generally speaking, PACI material has two types of magnetic anisotropy [11], namely out of plane anisotropy and easy magnetization plane anisotropy, respectively, which satisfy the fundamental conditions of the easy-plane anisotropy picture. Thus, the as-milled PACI particles can exceed Snoek's limit. Additionally, the PACI particles with a thickness smaller than their skin depth exhibit a higher complex permeability in a higher frequency range, as the eddy current effects is effectively restricted [12]. Zhang and his coworkers obtained de-aggregated flake-shaped carbonyl-iron particles by the high-energy planetary ball milling method and a higher permeability was obtained [13]. Recently, the permeability enhancement has been observed in flake-shaped Fe, FeCuNbSiB, Fe_3Co_2, etc. [14–17]. In this paper, we prepare flake-shaped particles with planar anisotropy by a simple ball milling technique and investigate the high frequency complex permeability of PACI/paraffin composite.

Furthermore, according to previous results [18–21], an enhancement of permeability is obtained after the flake-shaped particles are rotationally oriented in an external magnetic field. Here, we use this method to prepare PACI/paraffin composite with rotational orientation, and present the comparison of complex permeability between the oriented and non-oriented PACI composites.

2. Experimental procedure

The raw carbonyl-iron powder purchased from Tianyi super-fine metallic powder Co. Ltd. Jiangsu province, China, which is manufactured by decomposition of $Fe(CO)_5$ in the gaseous state. The raw powder was milled on a planetary ball mill with 200 rpm and 500 rpm for 8 h to obtain PACI particles. In ball milling process 50 ml n-hexane was added as the process control agent. The ball-to-powder weight ratio was 25:1.

The paraffin composites were prepared by mixing particles and paraffin with 50% volume concentration of the particles. The mixture was pressed into a toroidal-shape with an outer diameter of 7 mm, an inner diameter of 3.04 mm, and a length of 1.5–3.0 mm for microwave measurement. The oriented composite was fabricated with a simple rotational orientation method, in which the powder was first mixed with warm and molten paraffin wax, and then the suspension was placed in an applied magnetic field and ceaselessly rotated until the paraffin wax solidified. Through the rotational orientation, the flake planes of the particles were perpendicular to the axial direction of the toroidal samples.

The complex permeability of the coaxial samples was obtained using an Agilent E8363B vector network analyzer in the 0.1–18 GHz range. The static magnetic properties of particles were measured using a vibrating sample magnetometer (VSM Lakeshore 7304). The morphology of the samples was analyzed by scanning electron microscope (SEM HITACHI S-4800). The planar anisotropy property of the as-milled particles was characterized by room temperature transmission Mössbauer spectra. In the transmission geometry, the incident γ-ray is parallel to the axis of the oriented disk.

3. Results and discussion

The morphological change of carbonyl-iron particles after ball milling is shown in Fig. 2. The raw iron powders have a spherical shape with a size distribution of 1–5 μm. With increasing of ball milling speeds, the raw powders are deformed into thin flake particles. After ball milling SSCI particles with 200 rpm for 8 h, there are still many spherical particles besides the flakes with the thickness of 500 nm. After ball milling with 500 rpm, the raw particles are almost deformed into thin flake particles and the typical thickness is approximate 100 nm, which is far less than the skin depth of carbonyl-iron (about 1 μm in the 1–5 GHz range) [22].

The magnetic hysteresis loops of SSCI and PACI particles in Fig. 4 were measured at room temperature between −12 KOe and 12 KOe, which exhibit that all three samples have excellent soft magnetic properties. The saturation magnetization (M_s) of SSCI particles and PACI particles with 200 rpm and 500 rpm is 215.3 emu/g, 203.8 emu/g and 190.4 emu/g. The saturation magnetization of PACI particles occurred at a much smaller field. It means that

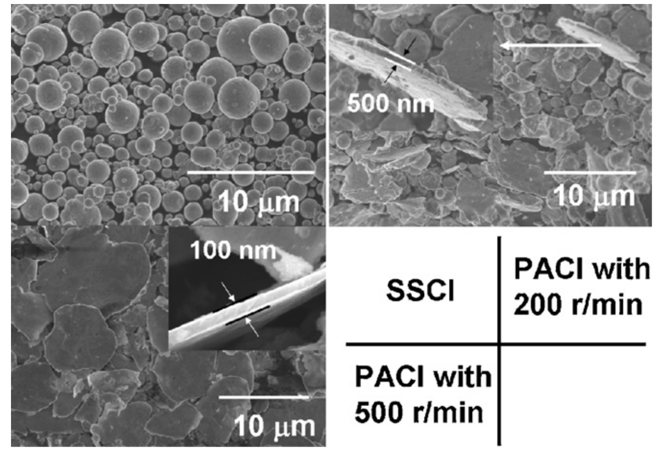

Fig. 2. SEM images of SSCI, PACI with 200 rpm and 500 rpm particles.

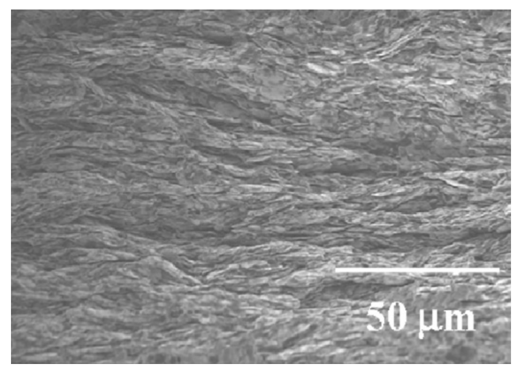

Fig. 3. SEM image of the fractured cross-sections of the oriented disk-shaped samples (500 rpm).

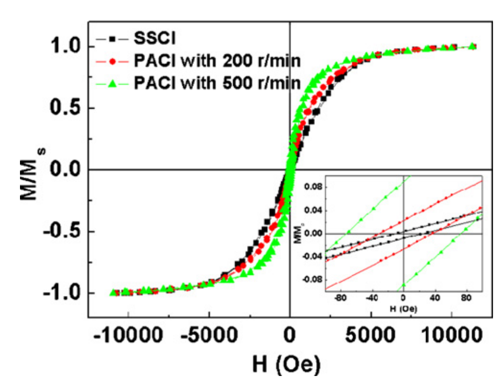

Fig. 4. Hysteresis loops of SSCI and PACI particles.

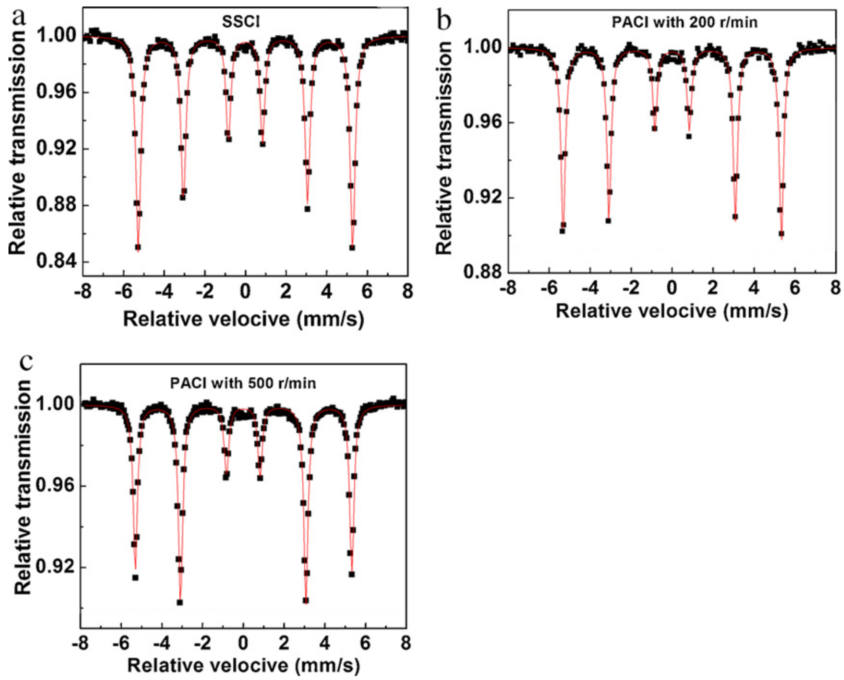

Fig. 5. Mössbauer spectra of SSCI/paraffin composite (a), oriented disk-shaped PACI/paraffin composite (50%, vol%), PACI particles milled with 200 rpm (b) and 500 rpm (c) at room temperature.

the static permeability is higher than that of SSCI particles. The coercive forces H_c for the three samples are about 12.0 Oe, 31.6 Oe and 70.4 Oe. The enhancement of the coercivity H_c is originated from the disordered crystal structure of as-milled powders due to the increasing internal strain by ball milling process [21].

Fig. 5 shows the Mössbauer spectra of oriented disk-shaped PACI composite produced by milling with 200 rpm and 500 rpm, respectively. The experimental data are fitted by a magnetic splitting sextet. The hyperfine fields of the two kinds of PACI composites are both 33.0 T, which is the same as the bulk of α-iron. In Mössbauer experiments, the average angle (β) between the incident γ-ray and the magnetization direction can be expressed by the relative intensity ratio [23]:

$$\frac{I_{2,5}}{I_{1,6}} = \frac{4\sin^2\beta}{3(1+\cos^2\beta)}, \quad (3)$$

where $I_{2,5}$ and $I_{1,6}$ are the relative intensity of the 2, 5 and 1, 6 peaks in magnetic splitting sextet, respectively. When the magnetic moments of the resonance atom ^{57}Fe, which can be detected, are distributed randomly, the ratio between 2, 5 and 1, 6 peaks is 2/3 (see Fig. 5(a)). For the oriented disk, the relative intensity ratios $I_{2,5}/I_{1,6}$ for two kinds of PACI particles are 0.89 and 1.17, the angles (β) calculated from formula (1) between the incident γ-ray and the magnetization direction are 63.6° and 75.29°, respectively. These results demonstrate that the as-milled PACI particles possess planar anisotropy and the increase of ball milling speeds results in an enhancement of planar anisotropy.

The complex permeability ($\mu_i = \mu' + i\mu''$) of paraffin composites with 50% volume concentration of the particles was evaluated by measuring the reflection coefficient S_{11} and the transmission coefficient S_{21} in an APC7 coaxial mode. Fig. 6 shows the frequency-dependent complex permeability of SSCI composite and PACI composites with 200 rpm and 500 rpm in the 0.1–18 GHz range. It is evident that the complex permeability of PACI samples is much higher than that of SSCI one. The real part of complex permeability μ' for PACI composites are 8.7 and 8.6 at 0.1 GHz, respectively, whereas that of SSCI composite is 6.1. The imaginary part of complex permeability μ'' for the three kinds of samples increases from 0.3, 0.1 and 0.4 to 2.0, 3.5 and 5.3 in the range of 0.1–3.5 GHz, 0.1–3.7 GHz, and 0.1–4.3 GHz, respectively, and then decreases in the higher frequency range. The flake-shaped carbonyl-iron particles with planar anisotropy exhibit a higher permeability in a higher frequency range compared with the isotropy ones. This is due to the ratio of thickness to averaged diameter is smaller than 1/10, while the conventional fillers are spherical in shape. On the other hand, the fillers have larger dimensions in sizes but are still much smaller than the wavelength of EM wave, while the conventional fillers are fine particles with diameters of 1–5 μm. Additionally, the eddy current effects are effectively suppressed as the thickness of the flaky particles is smaller than their skin depth. The attenuated permeability for PACI particles with 200 rpm may be due to the change of aspect ratio. The enhancement of aspect ratio results in a decrease of eddy current effects [24,25]. The shift of the resonance frequency towards higher frequency range is attributed to the increase of planar anisotropy (see Mössbauer results). As the ball milling speed increases, the planar anisotropy fields add to the total anisotropy field and consequently increases the resonance frequency.

The effective static permeability ($\mu_{s,e}$) of composite is defined as the real permeability at frequency of 0.1 GHz. The resonance frequency (f_r) is defined as the corresponding frequency for the maximum imaginary permeability. According to the Bruggeman's

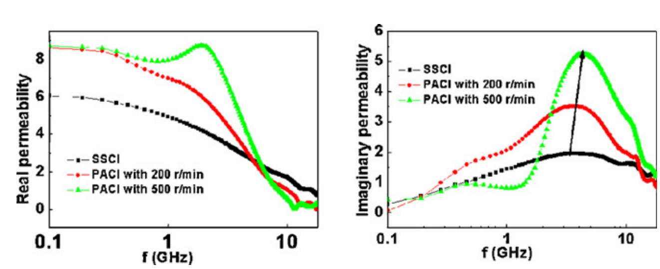

Fig. 6. The real (left) and the imaginary (right) magnetic permeability spectra for SSCI composite and PACI composites with 200 rpm and 500 rpm.

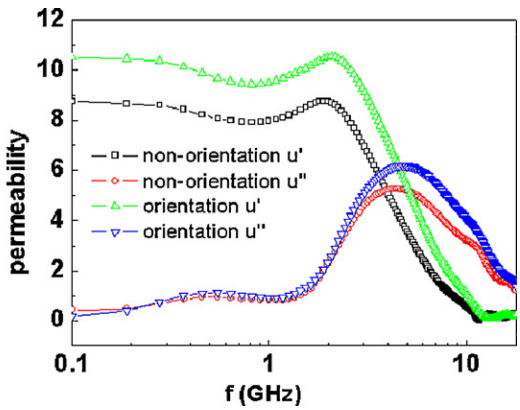

Fig. 7. The complex permeability spectra of PACI composites (500 rpm) with and without rotational orientation.

effective medium theory [26], the static permeability of PACI composite (500 rpm) is approximate 27.5, and the resonance frequency is 4.3 GHz. The product of the static permeability and the resonance frequency for PACI particles is 114.0 GHz, which is much higher than the Snoek's constant 40 GHz for isotropy carbonyl-iron particles. This result demonstrates that the intrinsic high frequency magnetic properties of the PACI particles exceed the Snoek's limit.

Fig. 7 presents the complex permeability of PACI composite (500 rpm) with and without rotational orientation. There is a remarkable feature that both μ' and μ'' of the oriented sample are larger than those of non-oriented one. The real part of permeability μ' for the oriented composite reaches a large value of approximate 10.5 at 0.1 GHz, whereas that of the non-oriented one is 8.7. There is an exceptional increasing by an average factor of 1.2, which is in good agreement with Ref. [21]. According to Ref. [21], oriented iron-based amorphous-metal flakes system shows 1.2–1.5 times higher values of complex permeability than that without orientation [21]. From our Mössbauer measurement (see Fig. 5(b) and (c)) we know that magnetic moments lie preferentially in the plane of the flake due to demagnetization effect. The rotational orientation in an external magnetic field induces that all the planes of flakes in the composite are perpendicular to the normal of the oriented disk (Fig. 3). The parallel arrangement of easy planes of the particles results in the higher permeability [27,28]. On the other hand, the imaginary part of permeability μ'' of the oriented sample has a wider resonance peak and the resonance frequency shifts to the higher frequency range compared with that of the non-oriented one. The mean value of about 4.0 in a broad frequency range from 2.5 GHz to 10.6 GHz, whereas that of the non-oriented one is from 2.7 GHz to 7.6 GHz. The increase of resonance frequency after rotational orientation is considered as being a direct consequence of the increase of the microscopic demagnetizing fields in the mixture in connection with the modifications of dipolar-type interactions [29].

4. Conclusion

In summary, we have investigated the microwave complex permeability of as-milled PACI particles embedded in paraffin with 50% volume concentration of particles. The as-milled PACI composites exhibit a dramatic enhancement of complex permeability and a higher resonance frequency compared with SSCI composite, and thus the intrinsic high frequency magnetic properties of the as-milled particles with planar anisotropy exceed Snoek's limit. The value of the complex permeability is further increased when the composite containing PACI particles is rotationally oriented in an external magnetic field. This work suggests that as-milled particles with planar anisotropy can serve as a good high frequency soft magnetic material.

Acknowledgment

This work was supported by the National Natural Science Foundation of China under contract no. 10774061.

References

[1] Y.C. Qing, W.C. Zhou, F. Luo, D.M. Zhu, J. Magn. Magn. Mater. 321 (2009) 25–28.
[2] Y.B. Feng, T. Qiu, C.Y. Shen, X.Y. Li, IEEE Trans. Magn. 42 (2006) 363–368.
[3] J.R. Liu, M. Itoh, T. Horikawa, M. Itakura, N. Kuwano, K.-I. Machida, J. Phys. D: Appl. Phys. 37 (2004) 2737–2741.
[4] J.R. Liu, M. Itoh, K.-I. Machida, Appl. Phys. Lett. 83 (2003) 4017–4019.
[5] F.S. Wen, L. Qiao, H.B. Yi, D. Zhou, F.S. Li, Chin. Phys. Lett. 25 (2008) 751–754.
[6] Y.X. Gong, L. Zhen, J.T. Jiang, C.Y. Xu, W.Z. Shao, J. Appl. Phys. 106 (2009) 064302–064305.
[7] J.L. Snoek, Physica 14 (1948) 207–217.
[8] R. Lebourgeois, C.L. Fur, M. Labeyrie, M. Pate, J.P. Ganne, J. Magn. Magn. Mater. 160 (1996) 329–332.
[9] T.L. Gilbert, IEEE Trans. Magn. 40 (2004) 3443–3449.
[10] D.S. Xue, F.S. Li, X.L. Fan, F.S. Wen, Chin. Phys. Lett. 25 (2008) 4120.
[11] F.S. Wen, L. Qiao, D. Zhou, W.L. Zuo, H.B. Yi, F.S. Li, Chin. Phys. B 17 (2008) 2263–2267.
[12] P.H. Zhou, J.L. Xie, Y.Q. Liu, L.J. Deng, J. Magn. Magn. Mater. 320 (2008) 3390–3393.
[13] B.S. Zhang, Y. Feng, J. Xiong, Y. Yang, H. Lu, IEEE Trans. Magn. 42 (0018–9464) (2006) 1778–1781.
[14] M.A. Abshinova, A.V. Lopatin, N.E. Kazantseva, J. Vilcáková, P. Sáha, Comp. A: Appl. Sci. Manuf. 38 (12) (2007) 2471–2485.
[15] F.S. Wen, W.L. Zuo, H.B. Yi, N. Wang, L. Qiao, F.S. Li, Phys. B: Condens. Matter. 404 (20) (2009) 3567–3570.
[16] L. Qiao, F.S. Wen, J.Q. Wei, J.B. Wang, F.S. Li, J. Appl. Phys. 103 (6) (2008) 063903–063905.
[17] P.H. Zhou, L.J. Deng, J.L. Xie, D.F. Liang, J. Alloys Compd. 448 (2008) 303–307.
[18] J. Smit, H.P.J. Wijn, Ferrites, Philips Technical Library, Eindhoven, 1959.
[19] H. Su, H. Zhang, X. Tang, Y. Jing, Z. Zhong, J. Alloys Compd. 481 (2009) 841–844.
[20] W.F. Yang, L. Qiao, J.Q. Wei, Z.Q. Zhang, T. Wang, F.S. Li, J. Appl. Phys. 107 (2010) 033913.
[21] M. Matsumoto, Y. Miyata, IEEE Trans. Magn. 33 (1997) 4459–4464.
[22] J.R. Liu, M. Itoh, K.-I. Machida, Appl. Phys. Lett. 88 (2006) 062503.
[23] M. Kopcewicz, T. Lucinski, F. Stobiecki, G. Reiss, J. Appl. Phys. 85 (1999) 5039–5041.
[24] X. Wang, R. Gong, P. Li, L. Liu, W. Cheng, Mater. Sci. Eng. A 466 (2007) 178–182.
[25] H.S. Cho, A.S. Kim, S.M. Kim, J. Namgung, M.C. Kim, G.A. Lee, Physica Status Solidi (a) 201 (2004) 1942–1945.
[26] L.Z. Wu, J. Ding, H.B. Jiang, C.P. Neo, L.F. Chen, C.K. Ong, J. Appl. Phys. 99 (2006) 083905–83907.
[27] Y. Shirakata, N. Hidaka, M. Ishitsuka, A. Teramoto, T. Ohmi, IEEE Trans. Magn. 44 (2008) 2100–2106.
[28] Z.W. Li, Z.H. Yang, L.B. Kong, Appl. Phys. Lett. 96 (2010) 092507–92513.
[29] A. Chevalier, F.M. Le, J. Appl. Phys 90 (2001) 3462–3465.